

# Large exchange bias and its connection to interface structure in FeF<sub>2</sub>-Fe bilayers

J. Nogués,<sup>a)</sup> D. Lederman,<sup>b)</sup> T. J. Moran, and Ivan K. Schuller  
*Physics Department 0319, University of California-San Diego, La Jolla, California 92093-0319*

K. V. Rao  
*Department of Condensed Matter Physics, Royal Institute of Technology, 10044 Stockholm, Sweden*

(Received 8 December 1995; accepted for publication 23 March 1996)

Large exchange bias effects ( $\Delta E \sim 1.1$  erg/cm<sup>2</sup>) were observed in antiferromagnetic (FeF<sub>2</sub>)-ferromagnetic (Fe) bilayers grown on MgO. The FeF<sub>2</sub> grows along the spin-compensated (110) direction. The FeF<sub>2</sub>-Fe interface roughness was characterized using specular and diffuse x-ray diffraction and atomic force microscopy. The magnitude of the exchange bias field  $H_E$  increases as the interface roughness decreases. These results imply that magnetic domain creation in the antiferromagnet plays an important role. © 1996 American Institute of Physics. [S0003-6951(96)02822-7]

Exchange anisotropy (EA), the interfacial interaction between a ferromagnet (FM) and an antiferromagnet (AF), produces a unidirectional interface coupling when a sample is field cooled across the AF Néel temperature. The shift of the FM hysteresis loop away from  $H=0$  is known as the exchange bias ( $H_E$ ). Technological applications include domain stabilizers in magnetoresistive heads and "spin-valve" based devices.<sup>1,2</sup> Despite extensive work,<sup>1-5</sup> many questions remain regarding the role of crystalline structure and interface disorder. We have studied the relationship between interface roughness and EA in FeF<sub>2</sub> (AF)-Fe (FM) bilayers. We find a large EA in fully compensated (zero net magnetic moment) FeF<sub>2</sub> surfaces and the highest  $H_E$  for the smoothest AF-FM interfaces. These samples have the highest EA energies ever reported for AF-FM bilayer *thin films* ( $\Delta E \sim 1.1$  erg/cm<sup>2</sup>), with a maximum  $H_E = 700$  Oe measured in a 6.7 nm thick Fe sample. Models based on domain wall creation in the AF are consistent with our results.

FeF<sub>2</sub> was chosen because of its simple rutile crystal structure, well-known spin structure (inset Fig. 1), and strong uniaxial magnetic anisotropy. Films were grown by sequential *e*-beam evaporations (pressure  $< 10^{-6}$  Torr) of FeF<sub>2</sub> ( $\sim 90$  nm at a rate of 0.2 nm/s) and Fe ( $\sim 12$  nm at a rate of 0.1 nm/s) on MgO (100) substrates. Substrates were heated to 450 °C for 900 s prior to deposition, then cooled to the FeF<sub>2</sub> growth temperature. The Fe layers were always deposited at 150 °C, and capped with  $\sim 9$  nm of Ag to prevent oxidation.

High angle  $\Theta - 2\Theta$  *ex situ* x-ray diffraction showed that the FeF<sub>2</sub> grows in the (110) orientation and that the Fe layer is polycrystalline with mainly (110) and (100) orientations. The full width at half-maximum of the (110) rocking curves,  $\Delta\Theta = 0.9 - 1.6^\circ$ , depends on the growth temperature.

Figure 1 shows the small angle specular x-ray diffraction (SXRD) for samples with the FeF<sub>2</sub> grown at different temperatures. High-frequency peaks correspond to the FeF<sub>2</sub>

thickness, while the low frequency envelope corresponds to Fe. Higher FeF<sub>2</sub> deposition temperatures result in lower amplitudes of high frequency peaks, due to an increase in the FeF<sub>2</sub> surface roughness and therefore larger film thickness fluctuations. Quantitative fits using the SUPREX program's<sup>6</sup> low-angle recursive optical model<sup>7</sup> adapted for trilayers are shown in Fig. 1. The roughness at the Fe-Ag interface increases with deposition temperature  $T_S$  (Table I), although two samples grown at  $T_S = 200$  °C have different interface roughness, perhaps due to different substrate roughness. Since the main difference between the samples is the FeF<sub>2</sub> growth temperature, the Fe-Ag interface roughness must be caused by roughness at the FeF<sub>2</sub>-Fe interface. We were unable to reproduce the curvature of the (IV)  $T_S = 300$  °C sample spectrum with our model.

To determine quantitatively the lateral correlation length

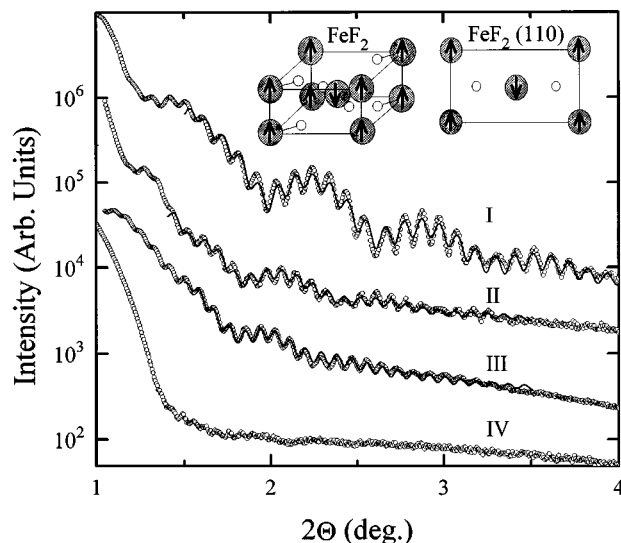


FIG. 1. Small angle x-ray diffraction ( $\lambda = 0.15418$  nm) for FeF<sub>2</sub> ( $\sim 90$  nm)-Fe ( $\sim 13$  nm)-Ag ( $\sim 9$  nm) samples with the FeF<sub>2</sub> grown at different temperatures  $T_S$ :  $T_S = 200$  °C (I), 200 °C (II), 250 °C (III), 300 °C (IV). Solid curves represent fits to optical x-ray model for samples I-III. Samples I and II are from different growth sessions. From top to bottom, fits yielded Fe-Ag interface roughnesses of 0.6, 1.0, and 1.5 nm. Inset: Bulk FeF<sub>2</sub> spin and crystal structure and the corresponding (110) surface spin structure.

<sup>a)</sup>On leave from the Grup d'Electromagnetisme, Universitat Autònoma de Barcelona, Spain.

<sup>b)</sup>Present address: Physics Department, West Virginia University, Morgantown, WV 26505-6315.

TABLE I. Fit results of specular x-ray diffraction (SXR), diffuse x-ray diffraction (DXRD), and atomic force microscopy (AFM) data. DXRD and AFM data were obtained in single FeF<sub>2</sub> films.  $\sigma$  is the vertical roughness and  $\xi$  the lateral correlation length of  $\sigma$ .

$T_S$ (°C)	$\sigma$ (nm)			$\xi$ (nm)	
	SXR	DXRD	AFM	DXRD	AFM
200	0.6±0.2	0.10±0.03	1.5±0.1	23±12	58±6
250	1.4±0.2		2.7±0.3		76±8
300		0.18±0.03	3.9±0.4	37±12	91±9

( $\xi$ ) of the vertical roughness ( $\sigma$ ), single FeF<sub>2</sub> films grown under the same conditions as above were studied by small angle diffuse x-ray diffraction (DXRD) and atomic force microscopy (AFM). Note that these techniques probe the structure at different length scales. DXRD data were analyzed using a model based on the Born approximation.<sup>8</sup> Variations in  $\chi^2$  were not large enough to reliably determine the fractal dimensionality  $h$ . However, for fixed values of  $h$ , samples grown at higher temperatures had larger average  $\sigma$  and  $\xi$ . The results for  $T_S = 200$  and 300 °C are shown in Table I and plotted in Fig. 2(a) for  $h = 0.5$ .  $\sigma$  was calculated from two-dimensional AFM scans by averaging the height fluctuations.  $\xi$  was determined by first calculating the two-dimensional height-height autocorrelation function, and then fitting the decay of the correlation function near  $R = 0$  to a Gaussian. As in the DXRD results, the AFM  $\sigma$  and  $\xi$  increase with  $T_S$  [Fig. 2(b) and Table I].

The magnetic characterization was performed using a superconducting quantum interference device magnetometer. Samples were cooled from 120 K through the FeF<sub>2</sub> Néel temperature ( $T_N = 78.4$  K), to 10 K in a magnetic field  $H_{fc}$ , large enough to saturate the FM layer, parallel to the film surface. The Fig. 3 inset shows hysteresis loops at

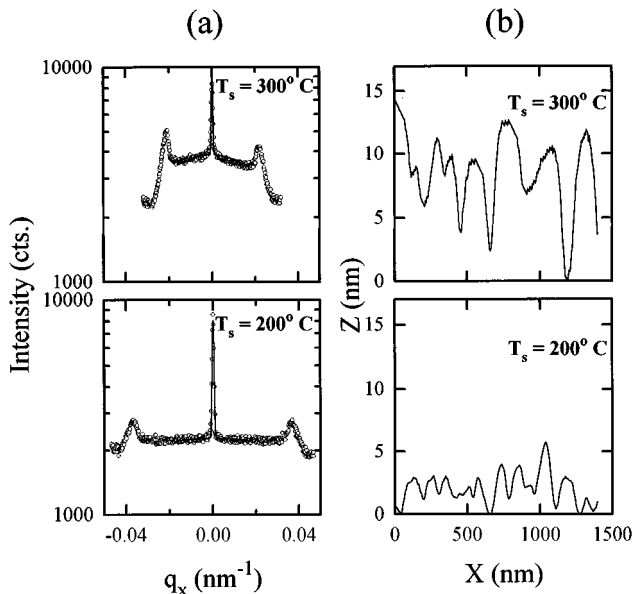


FIG. 2. (a) Diffuse x-ray scattering at  $q_z = 1.52$  nm<sup>-1</sup> and  $1.91$  nm<sup>-1</sup> for single FeF<sub>2</sub> films grown at  $T_S = 300$  °C and 200 °C, respectively. Solid curves represent fits to the model in Ref. 8 with a fixed  $h = 0.5$ . (b) Atomic force microscopy line scans for single FeF<sub>2</sub> samples grown on MgO at  $T_S = 300$  °C and 200 °C.

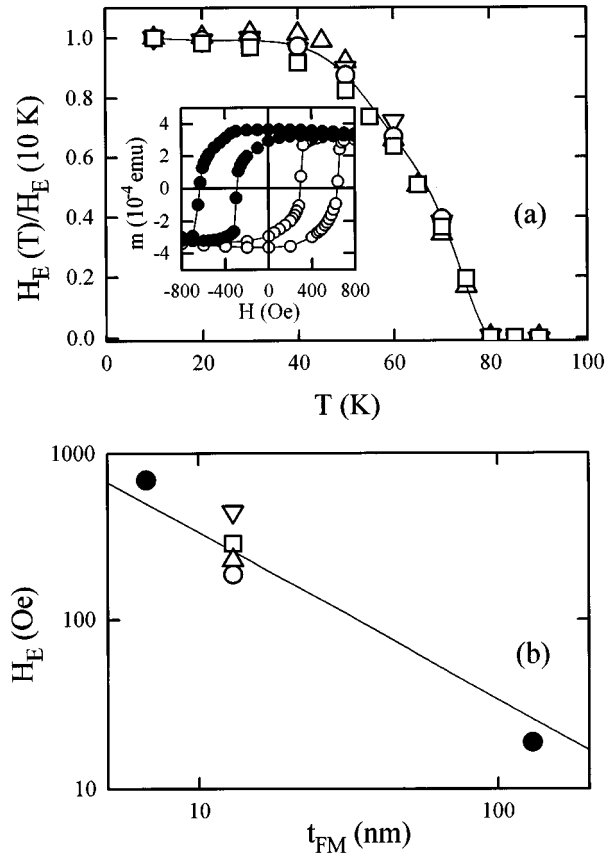


FIG. 3. Exchange bias  $H_E$  for samples I ( $\nabla$ ), II ( $\square$ ), III ( $\triangle$ ), and IV ( $\circ$ ) in Fig. 1. (a)  $H_E$  as a function of temperature normalized to  $H_E(10$  K). Inset: Hysteresis loops at  $T = 10$  K for FeF<sub>2</sub> (90 nm)–Fe (13 nm)–Ag (9 nm) grown at  $T_S = 200$  °C (sample I in Fig. 1) field cooled in 2000 Oe ( $\bullet$ ) and  $-2000$  Oe ( $\circ$ ). (b) Log-log plot of  $H_E(10$  K) as a function of Fe thickness  $t_{FM}$ . ( $\bullet$ ) are samples grown at  $T_S = 200$  °C with thicknesses of 6.7 and 130 nm.

$T = 10$  K for sample (I) cooled in positive and negative fields. Loops were measured in the temperature range  $10 < T < 120$  K for  $-H_{fc} < H < H_{fc}$ . Measuring several consecutive hysteresis loops had no effect on  $H_E$ .

The functional form of normalized  $H_E(T)$  is insensitive to the interface roughness, as illustrated in Fig. 3(a). However, the low temperature  $H_E$  reaches different maxima depending on interface roughness [Fig. 3(b)].  $H_E$  vanishes very close to  $T_N$  (i.e., the “blocking temperature”  $T_B$ , coincides with  $T_N$ ), in contrast with other thin film systems<sup>1,4</sup> where  $T_B < T_N$ . Together with the above surface analyses, this implies that the low temperature  $H_E$  increases as the AF–FM interface becomes smoother.

The magnitude of  $H_E$  is usually described in terms of an interface energy per unit area

$$\Delta E = M_{FM} t_{FM} H_E, \quad (1)$$

where  $M_{FM}$  and  $t_{FM}$  are the magnetization per unit volume and thickness of the ferromagnet respectively. Using the bulk Fe low-temperature saturation magnetization,  $M_{FM} = 1740$  Oe, our results are in the range  $0.2 < \Delta E < 1.1$  erg/cm<sup>2</sup>.

In the simplest microscopic model, with uncompensated AF surface fixed during the FM magnetization rotation,  $H_E$  is a result of the AF–FM interface exchange energy,<sup>3</sup>

$$\Delta E = \frac{2J_i S^2}{a^2}, \quad (2)$$

where  $J_i$  is the exchange at the interface,  $S$  is the spin, and  $a$  is the lattice parameter. Using the bulk Fe value,<sup>9</sup>  $\Delta E = 17 \text{ erg/cm}^2$ , more than one order of magnitude larger than our experimental results. Using the bulk  $\text{FeF}_2$  value,<sup>10</sup>  $\Delta E = 1.3 \text{ erg/cm}^2$ , is much closer to the experimental values.

More sophisticated models rely on the creation of AF domains either perpendicular to the interface, during the field cooling,<sup>11</sup> or parallel to the interface, during field reversal.<sup>12</sup>

The first of these models assumes a microscopically random exchange field at the interface, arising from defects, roughness, lattice mismatch, etc. For thick AF films

$$\Delta E = \frac{4zA_{\text{AF}}}{\sqrt{\pi}L}, \quad (3)$$

where  $z$  is a factor of order unity,  $A_{\text{AF}}$  is the AF exchange stiffness and  $L$  is the AF domain size. Taking  $L$  to be the domain wall size,  $L = \pi \sqrt{A_{\text{AF}}/K_{\text{AF}}}$ , with  $K_{\text{AF}}$  being the AF uniaxial anisotropy. Using  $\text{FeF}_2$   $K_{\text{AF}}$  and  $J_{\text{AF}}$  values,<sup>6</sup>  $\Delta E = 1.47 \text{ erg/cm}^2$ , of the same order of magnitude as our data. This model does not require an uncompensated AF surface, as long as an interfacial random exchange interaction exists which creates small, slightly uncompensated AF domains during cooling. The decrease in  $H_E$  could be due to a decrease in random exchange energy resulting from interactions between the FM and less favorable AF crystallographic directions. Moreover, the decrease in  $H_E$  could also be due to an increase in  $L$ , perhaps due to a lower number of defects in the AF because of the higher growth temperature. Finally, if  $\xi$  (Table I) is assumed to correspond to  $L$ , then  $H_E$  decreases with increasing  $T_S$  due to the lateral length scale of the interface disorder.

The second model assumes an AF with anisotropy and an *uncompensated* surface, forcing the creation of AF domain walls parallel to the interface during field reversal. This model predicts an upper limit for the exchange bias, corresponding to spin rotations of  $180^\circ$  away from the AF easy axis,

$$\Delta E = 2\sqrt{A_{\text{AF}}K_{\text{AF}}}. \quad (4)$$

For  $\text{FeF}_2$ ,  $\Delta E = 4.1 \text{ erg/cm}^2$ , of the same order of magnitude as our data. The observed  $H_E$  decrease with increasing interface roughness would be due to a weakening of the exchange interaction at the interface, thus decreasing the amount of AF spin rotation away from the AF easy axis. This model's ma-

ior deficiency in explaining our data is that it requires an uncompensated surface. However interface reconstruction could result in a net  $H_E$ .

Finally, the dependence of  $H_E$  on interface roughness seems to contradict recent work on permalloy films grown on  $\text{CoO}$  (111) single crystals.<sup>13</sup> This discrepancy may be due to differences in types of disorder, anisotropies, and favorable crystallographic directions.

In conclusion, we have prepared  $\text{FeF}_2$ -Fe bilayers, a new system exhibiting a large exchange anisotropy.  $H_E$  increases as the interfaces become smoother. This is surprising considering that the bulk  $\text{FeF}_2$  spin structure implies a magnetically compensated interface. Models which rely on AF domain creation are in agreement with these results.

We thank S. Sinha and J. M. Gallego for useful discussions, E. E. Fullerton for help with the SUPREX program, and V. Speriosu for motivating our initial interest in exchange anisotropy. This work was supported by the U. S. DOE and NSF. The development of the SUPREX program was supported by the U. S. DOE and the Belgian Interuniversity Attraction Pole Program. J.N. thanks the NATO Scientific Committee and the Spanish Ministerio de Educación y Ciencia for their financial support. After submission of this paper we became aware of large exchange anisotropy in ferrimagnetic-antiferromagnetic bilayers.<sup>5</sup>

<sup>1</sup>C. Tsang and R. Fontana, IEEE Trans. Magn. **18**, 1149 (1982).

<sup>2</sup>B. Dieny, J. Magn. Mater. **136**, 335 (1994).

<sup>3</sup>W. H. Meiklejohn and C. P. Bean, Phys. Rev. **105**, 904 (1957).

<sup>4</sup>W. C. Cain and M. H. Kryder, J. Appl. Phys. **67**, 5722 (1990); M. J. Carey and A. E. Berkowitz, Appl. Phys. Lett. **60**, 3060 (1992); R. Jungbult, R. Coehoorn, M. T. Johnson, C. Sauer, P. J. van der Zaag, A. R. Ball, T. G. S. M. Rijks, J. aan de Stegge, and A. Reinders, J. Magn. Mater. **148**, 300 (1995).

<sup>5</sup>P. J. van der Zaag, R. M. Wolk, A. R. Ball, C. Bordel, L. F. Feiner, and R. Jungbult, J. Magn. Mater. **148**, 346 (1995).

<sup>6</sup>I. K. Schuller, Phys. Rev. Lett. **44**, 1597 (1980); W. Sevenhans, M. Gijs, Y. Bruynseraede, H. Homma, and I. K. Schuller, Phys. Rev. B **34**, 5955 (1986); E. E. Fullerton, I. K. Schuller, H. Vanderstraeten, and Y. Bruynseraede, *ibid.* **45**, 9292 (1992).

<sup>7</sup>B. Vidal and P. Vincent, Appl. Opt. **23**, 1794 (1984).

<sup>8</sup>S. K. Sinha, E. B. Sirota, G. Garoff, and H. B. Stanley, Phys. Rev. B **38**, 2297 (1988).

<sup>9</sup>C. Kittel, *Introduction to Solid State Physics*, 6th ed. (Wiley, New York, 1986), p. 424.

<sup>10</sup>M. T. Hutchings, B. D. Rainford, and H. J. Guggenheim, J. Phys. C **3**, 307 (1970).

<sup>11</sup>A. P. Malozemoff, Phys. Rev. B **37**, 7673 (1988).

<sup>12</sup>D. Mauri, H. C. Siegmann, P. S. Bagus, and E. Kay, J. Appl. Phys. **62**, 3047 (1987).

<sup>13</sup>T. J. Moran, J. M. Gallego, and I. K. Schuller, J. Appl. Phys. **78**, 1887 (1995).